Micro-Station - Modal Analysis

Dehaeze Thomas

October 7, 2023

Contents

1 Measurement Setup **4**
- 1.1 Used Instrumentation . . . 4
- 1.2 Structure Preparation and Test Planing . . . 4
- 1.3 Location of the Accelerometers . . . 6
- 1.4 Hammer Impacts . . . 8
- 1.5 Force and Response signals . . . 8

2 Frequency Analysis **11**
- 2.1 First verification of the solid body assumption . . . 12
- 2.2 From accelerometer DOFs to solid body DOFs . . . 13
- 2.3 Frequency Response Matrix expressed at the Center of Mass . . . 15
- 2.4 Verify that we find the original FRF from the FRF in the global coordinates . . . 16

3 Modal Analysis **19**
- 3.1 Determine the number of modes . . . 19
- 3.2 Modal parameter extraction . . . 21
- 3.3 Obtained Mode Shapes animations . . . 24
- 3.4 Verify the validity of the Modal Model . . . 25

4 Conclusion **28**

Bibliography **29**

In order to properly make a multi-body model of the micro-station, an experimental modal-analysis is performed.

In fact, even though it is easy to estimate the inertia of each solid body from its geometry and its material density, it is much more difficult to properly estimate the stiffness and damping properties of the guiding elements connecting each solid body.

In this report, an experimental modal analysis is perform in order to ease the development of the multi-body model.

In Section 1 the measurement setup is presented. The instrumentation used (i.e. instrumented hammer, accelerometers and acquisition system) is presented, and obtained signals

Obtained frequency response functions between the forces applied using the instrumented hammer and the various accelerometers fixed to the structure are Section 2

Section 3

[1]

Table 1: Report sections and corresponding Matlab files

Sections	**Matlab File**
Section 1	`modal_1_meas_setup.m`
Section 2	`modal_2_frf_processing.m`
Section 3	`modal_3_analysis.m`

1 Measurement Setup

1.1 1.2 1.3 1.4 1.5

1.1 Used Instrumentation

In order to perform to **Modal Analysis** and to obtain first a **Response Model**, the following devices are used:

- An **acquisition system** (OROS) with 24bits ADCs (figure 1.1a)
- 3 tri-axis **Accelerometers** (figure 1.1b) with parameters shown on table 1.1
- An **Instrumented Hammer** with various Tips (figure 1.1c)

The acquisition system permits to auto-range the inputs (probably using variable gain amplifiers) the obtain the maximum dynamic range. This is done before each measurement. Anti-aliasing filters are also included in the system.

Table 1.1: 393B05 Accelerometer Data Sheet

Sensitivity	$10\,V/g$
Measurement Range	0.5 g pk
Broadband Resolution	4 µg rms
Frequency Range	0.7 to 450 Hz
Resonance Frequency	> 2.5 kHz

Tests have been conducted to determine the most suitable Hammer tip. This has been found that the softer tip gives the best results. It excites more the low frequency range where the coherence is low, the overall coherence was improved.

The accelerometers are glued on the structure.

1.2 Structure Preparation and Test Planing

All the stages are turned ON. This is done for two reasons:

- Be closer to the real dynamic of the station in used

(a) OROS acquisition system

(b) Accelerometer (M393B05)

(c) Instrumented Hammer

Figure 1.1: Instrumentation used for the modal analysis

- If the control system of stages are turned OFF, this would results in very low frequency modes un-identifiable with the current setup, and this will also decouple the dynamics which would not be the case in practice

This is critical for the translation stage and the spindle as their is no stiffness in the free DOF (air-bearing for the spindle for instance).

The alternative would have been to mechanically block the stages with screws, but this may result in changing the modes.

The stages turned ON are:

- Translation Stage
- Tilt Stage
- Spindle and Slip-Ring
- Hexapod

The top part representing the NASS and the sample platform have been removed in order to reduce the complexity of the dynamics and also because this will be further added in the model inside Simscape.

All the stages are moved to their zero position (Ty, Ry, Rz, Slip-Ring, Hexapod).

All other elements have been remove from the granite such as another heavy positioning system.

The goal is to identify the full $N \times N$ FRF matrix H (where N is the number of degree of freedom of the system):

$$H_{jk} = \frac{X_j}{F_k} \tag{1.1}$$

However, from only one column or one line of the matrix, we can compute the other terms thanks to the principle of reciprocity.

Either we choose to identify $\frac{X_k}{F_i}$ or $\frac{X_i}{F_k}$ for any chosen k and for $i = 1, \ ..., \ N$.

We here choose to identify $\frac{X_i}{F_k}$ for practical reasons:

- it is easier to glue the accelerometers on all the stages and excite only a one particular point than doing the opposite

The measurement thus consists of:

- always excite the structure at the same location with the Hammer
- Move the accelerometers to measure all the DOF of the structure

We will measured 3 columns (3 impacts location) in order to have some redundancy and to make sure that all modes are excited.

1.3 Location of the Accelerometers

4 tri-axis accelerometers are used for each solid body.

Only 2 could have been used as only 6DOF have to be measured, however, we have chosen to have some **redundancy**.

This could also help us identify measurement problems or flexible modes is present.

The position of the accelerometers are:

- 4 on the first granite
- 4 on the second granite
- 4 on top of the translation stage (figure 1.2a)
- 4 on top of the tilt stage
- 3 on top of the spindle
- 4 on top of the hexapod (figure 1.2b)

In total, 23 accelerometers are used: **69 DOFs are thus measured**.

The precise determination of the position of each accelerometer is done using the SolidWorks model (shown on figure 1.3).

The precise position of all the 23 accelerometer with respect to a frame located at the point of interest (located 270mm above the top platform of the hexapod) are shown in table 1.2.

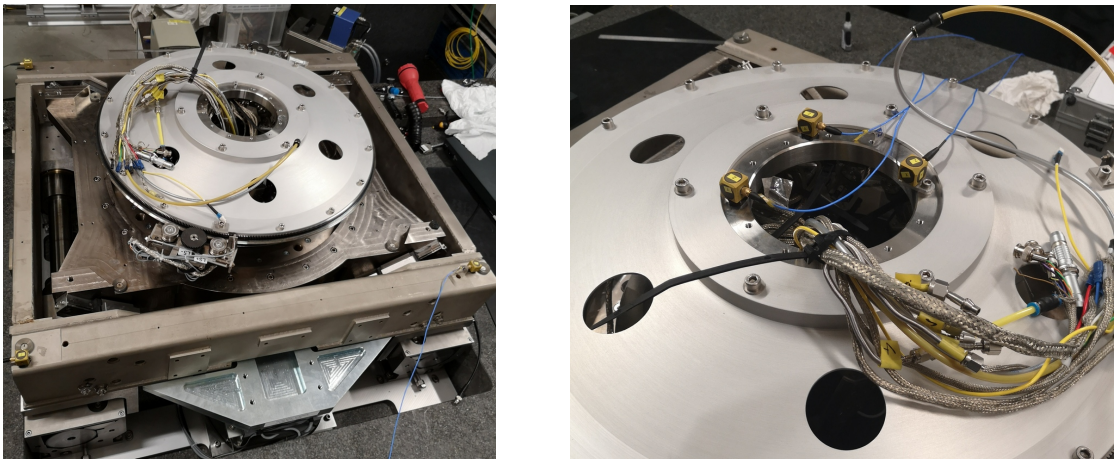

(a) T_y stage **(b)** Micro-Hexapod

Figure 1.2: Accelerometers fixed on the micro-station

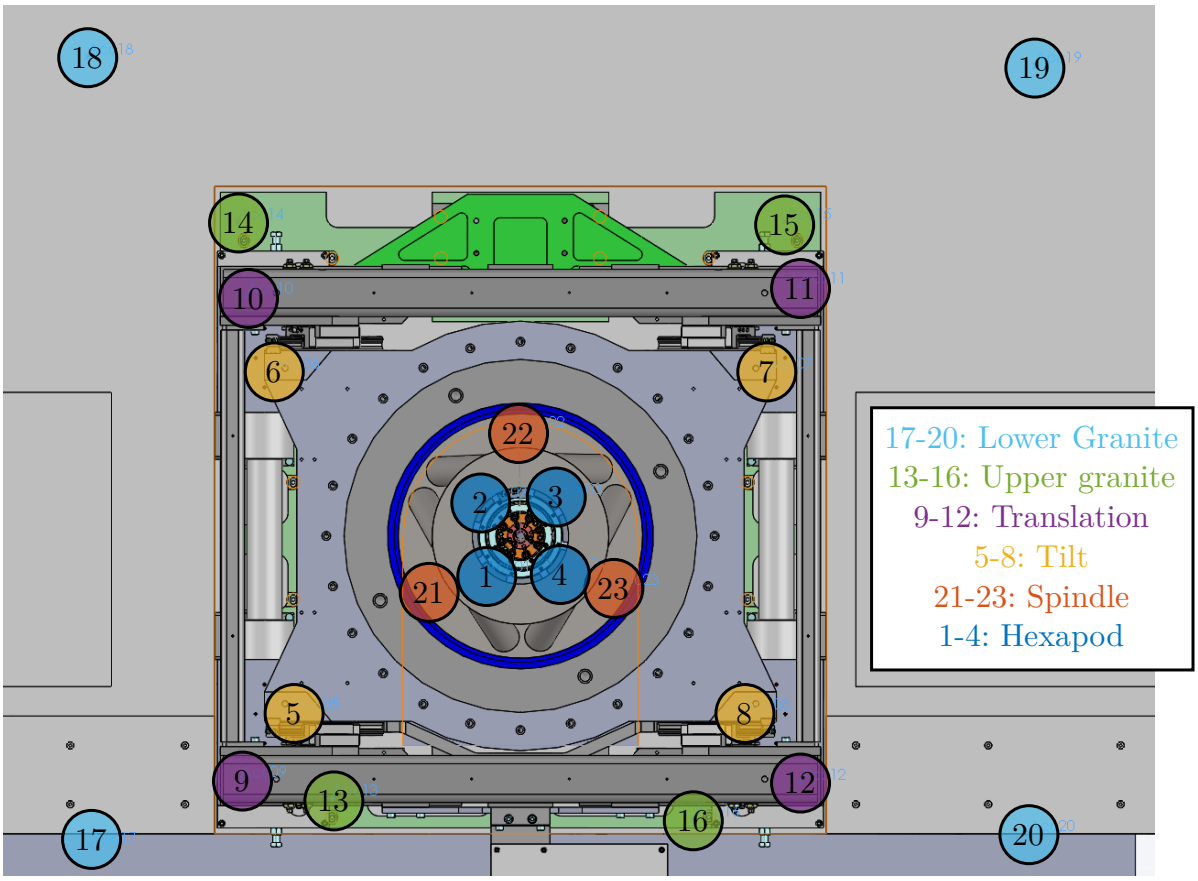

Figure 1.3: Position of the accelerometers using SolidWorks

Table 1.2: Position of the accelerometers

	ID	x [mm]	y [mm]	z [mm]
Hexapod	1	-64	-64	-270
Hexapod	2	-64	64	-270
Hexapod	3	64	64	-270
Hexapod	4	64	-64	-270
Tilt	5	-385	-300	-417
Tilt	6	-420	280	-417
Tilt	7	420	280	-417
Tilt	8	380	-300	-417
Translation	9	-475	-414	-427
Translation	10	-465	407	-427
Translation	11	475	424	-427
Translation	12	475	-419	-427
Upper Granite	13	-320	-446	-786
Upper Granite	14	-480	534	-786
Upper Granite	15	450	534	-786
Upper Granite	16	295	-481	-786
Lower Granite	17	-730	-526	-951
Lower Granite	18	-735	814	-951
Lower Granite	19	875	799	-951
Lower Granite	20	865	-506	-951
Spindle	21	-155	-90	-594
Spindle	22	0	180	-594
Spindle	23	155	-90	-594

1.4 Hammer Impacts

Only 3 impact points are used. The impact points are shown on figures 1.4a, 1.4b and 1.4c.

We chose this excitation point as it seems to excite all the modes in the frequency band of interest and because it provides good coherence for all the accelerometers.

From [1]: Most modal test require a point mobility measurement as one of the measured FRF. This is hard to achieve as both force and response transducer should be at the same point on the structure.

1.5 Force and Response signals

The force sensor and the accelerometers signals are shown in the time domain in Figure 1.5. Sharp "impacts" can be seen for the force sensor, indicating wide frequency band excitation. For the accelerometer, many resonances can be seen on the right, indicating complex dynamics

The "normalized" amplitude spectral density of the two signals are computed and shown in Figure 1.6. Conclusions based on the time domain signals can be clearly seen in the frequency domain (wide frequency content for the force signal and complex dynamics for the accelerometer).

The frequency response function from the applied force to the measured acceleration can then be computed (Figure 1.7).

The coherence between the input and output signals is also computed and found to be good between 20 and 200Hz (Figure 1.8).

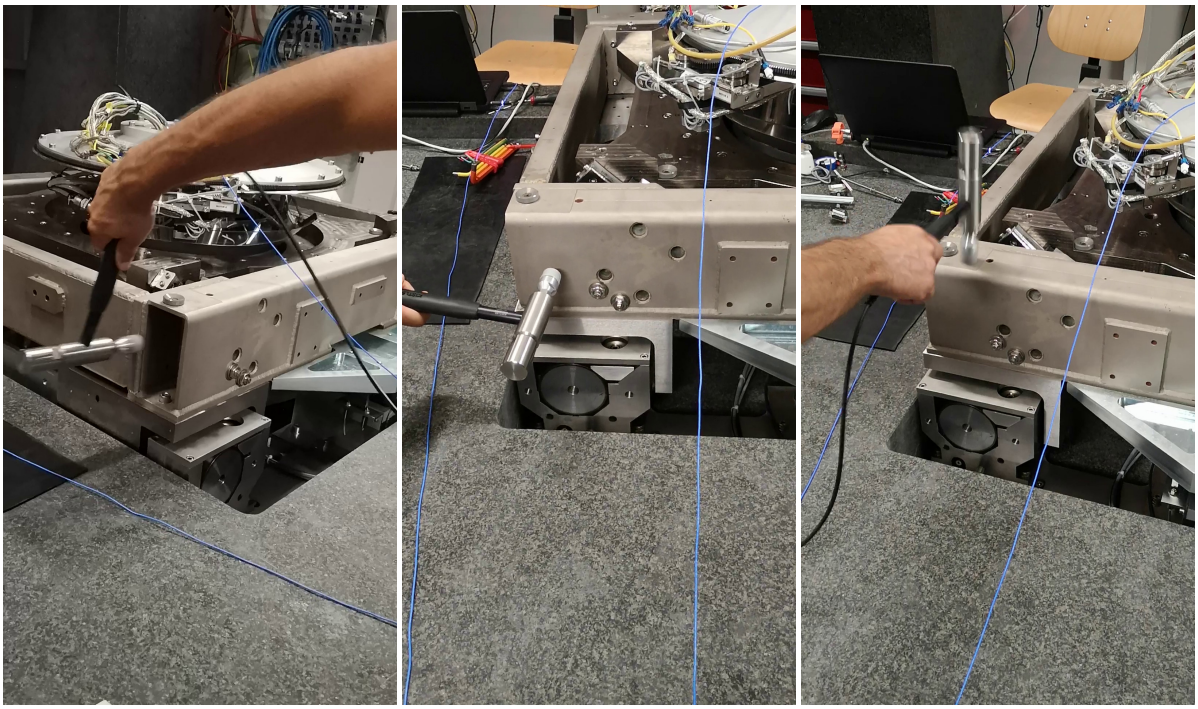

(a) X impact **(b)** Y impact **(c)** Z impact

Figure 1.4: The three hammer impacts used for the modal analysis

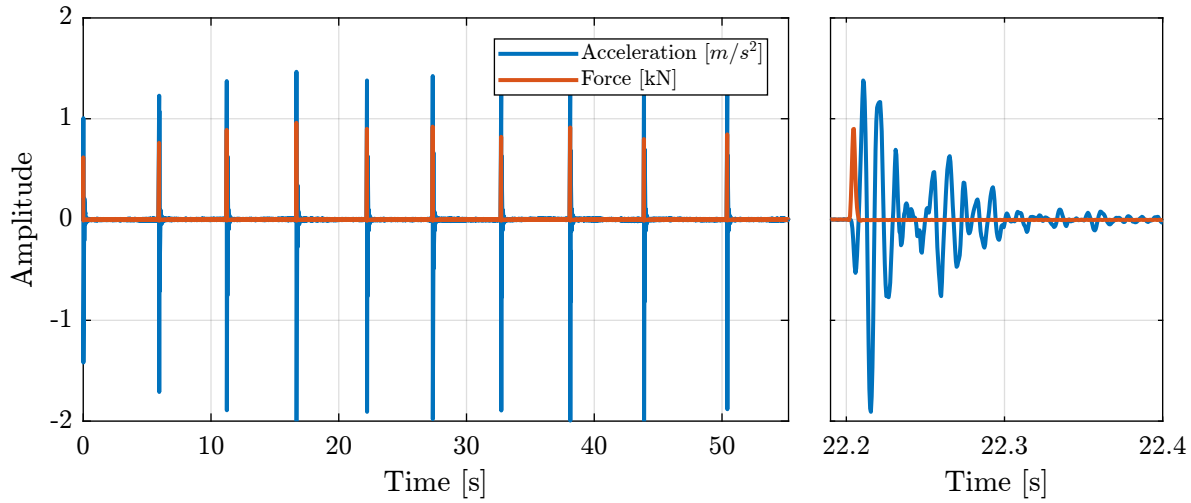

Figure 1.5: Raw measurement of the acceleromter (blue) and of the force sensor at the Hammer tip (red). Zoom on one impact is shown on the right.

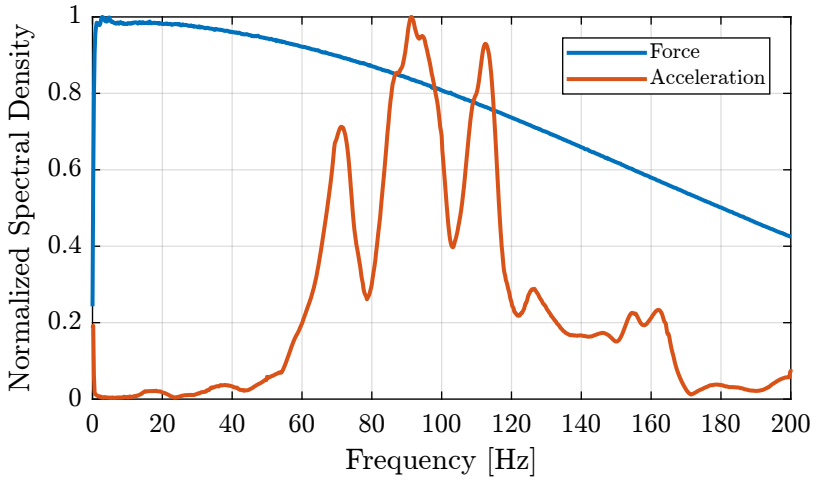

Figure 1.6: Normalized Amplitude Spectral Density of the measured force and acceleration

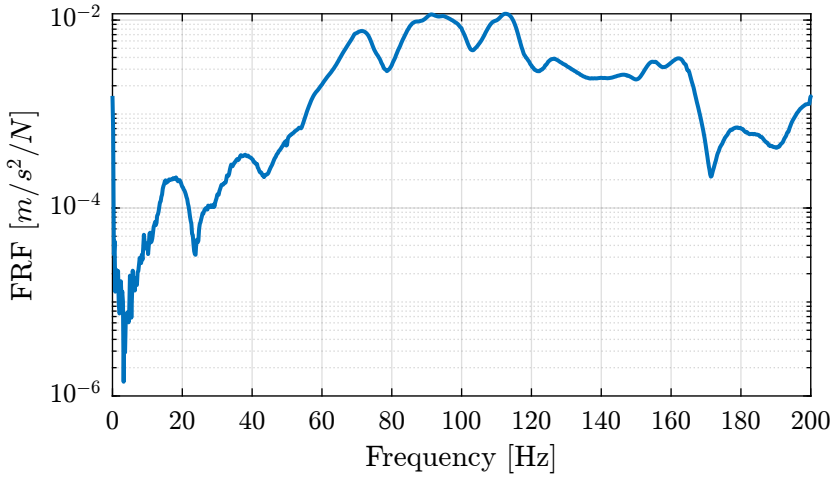

Figure 1.7: Frequency Response Function between the measured force and acceleration

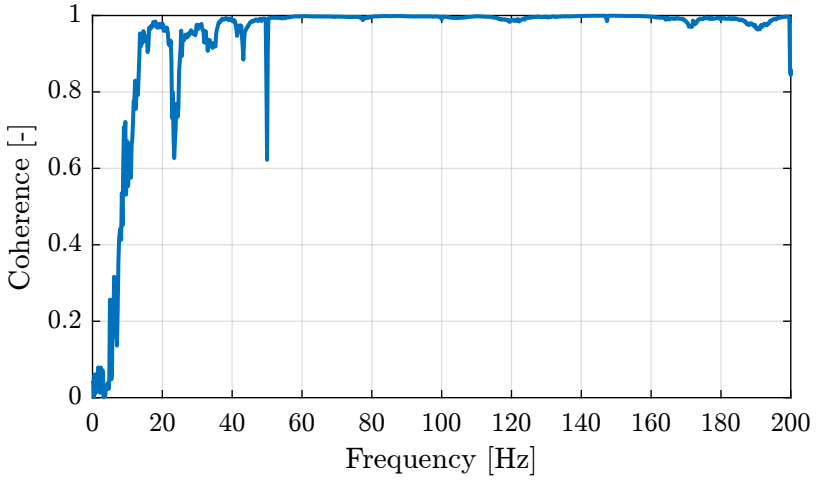

Figure 1.8: Coherence between the measured force and acceleration

2 Frequency Analysis

The measurements have been conducted and a $n \times p \times q$ Frequency Response Functions Matrix has been computed with:

- n: the number of output measured accelerations: $23 \times 3 = 69$ (23 accelerometers measuring 3 directions each)
- p: the number of input force excitations: 3
- q: the number of frequency points ω_i

Thus, the FRF matrix is an $69 \times 3 \times 801$ matrix.

For each frequency point ω_i, a 2D matrix is obtained that links the 3 force inputs to the 69 output accelerations:

$$\text{FRF}(\omega_i) = \begin{bmatrix} \frac{D_{1_x}}{F_x}(\omega_i) & \frac{D_{1_x}}{F_y}(\omega_i) & \frac{D_{1_x}}{F_z}(\omega_i) \\ \frac{D_{1_y}}{F_x}(\omega_i) & \frac{D_{1_y}}{F_y}(\omega_i) & \frac{D_{1_y}}{F_z}(\omega_i) \\ \frac{D_{1_z}}{F_x}(\omega_i) & \frac{D_{1_z}}{F_y}(\omega_i) & \frac{D_{1_z}}{F_z}(\omega_i) \\ \frac{D_{2_x}}{F_x}(\omega_i) & \frac{D_{2_x}}{F_y}(\omega_i) & \frac{D_{2_x}}{F_z}(\omega_i) \\ \vdots & \vdots & \vdots \\ \frac{D_{23_z}}{F_x}(\omega_i) & \frac{D_{23_z}}{F_y}(\omega_i) & \frac{D_{23_z}}{F_z}(\omega_i) \end{bmatrix} \tag{2.1}$$

However, for the multi-body model being developed, only 6 solid bodies are considered, namely: the bottom granite, the top granite, the translation stage, the tilt stage, the spindle and the hexapod. Therefore, only $6 \times 6 = 36$ degrees of freedom are of interest.

The objective in this section is therefore to process the Frequency Response Matrix to reduce the number of measured DoFs from 69 to 36.

In order to be able to perform this reduction of measured DoFs, the measures stages have to behave as rigid bodies in the frequency band of interest. This

2.1

To go from the accelerometers DoFs to the solid body 6 DoFs (three translations and three rotations), some computations have to be performed. This is explained in Section 2.2.

Finally, the $69 \times 3 \times 801$ frequency response matrix is reduced to a $36 \times 3 \times 801$ frequency response matrix where the motion of each solid body is expressed with respect to the CoM of the solid body (Section 2.3).

To validate this reduction of DoF and the solid body assumption, the frequency response function at the

accelerometer location are synthesized from the reduced frequency response matrix and are compared with the initial measurements in Section 2.4.

2.1 First verification of the solid body assumption

In this section, it is shown that two accelerometers fixed to a rigid body at positions $\vec{p}_1$ and $\vec{p}_2$ in such a way that $\vec{p}_2 = \vec{p}_1 + \alpha\vec{x}$ will measure the same value in the $\vec{x}$ direction. Such situation is illustrated on Figure 2.1 and is the case for many accelerometers as shown in Figure 1.3.

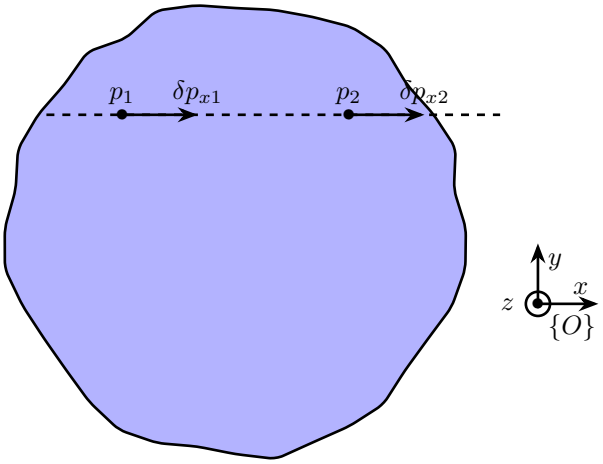

Figure 2.1: Aligned measurement of the motion of a solid body

The motion of the rigid body of figure 2.1 can be defined by its displacement $\delta\vec{p}$ and rotation $\vec{\Omega}$ with respect to a reference frame $\{O\}$.

The motions at points 1 and 2 are:

$$\delta\vec{p}_1 = \delta\vec{p} + \vec{\Omega} \times \vec{p}_1$$
$$\delta\vec{p}_2 = \delta\vec{p} + \vec{\Omega} \times \vec{p}_2$$

Taking only the x direction:

$$\delta p_{x1} = \delta p_x + \Omega_y p_{z1} - \Omega_z p_{y1}$$
$$\delta p_{x2} = \delta p_x + \Omega_y p_{z2} - \Omega_z p_{y2}$$

However, we have $p_{1y} = p_{2y}$ and $p_{1z} = p_{2z}$ because of the co-linearity of the two sensors in the x direction, and thus we obtain:

$$\boxed{\delta p_{x1} = \delta p_{x2}} \tag{2.2}$$

It is therefore concluded that two position sensors fixed to a rigid body will measure the same quantity in the direction "linking" the two sensors.

Such property can be used to verify that the considered stages are indeed behaving as rigid body in the frequency band of interest.

From Table 1.2, we can identify which pair of accelerometers are aligned in the X and Y directions.

The response in the X direction of pairs of sensors aligned in the X direction are compared in Figure 2.2. Good match is observed up to 200Hz. Similar result is obtained for the Y direction.

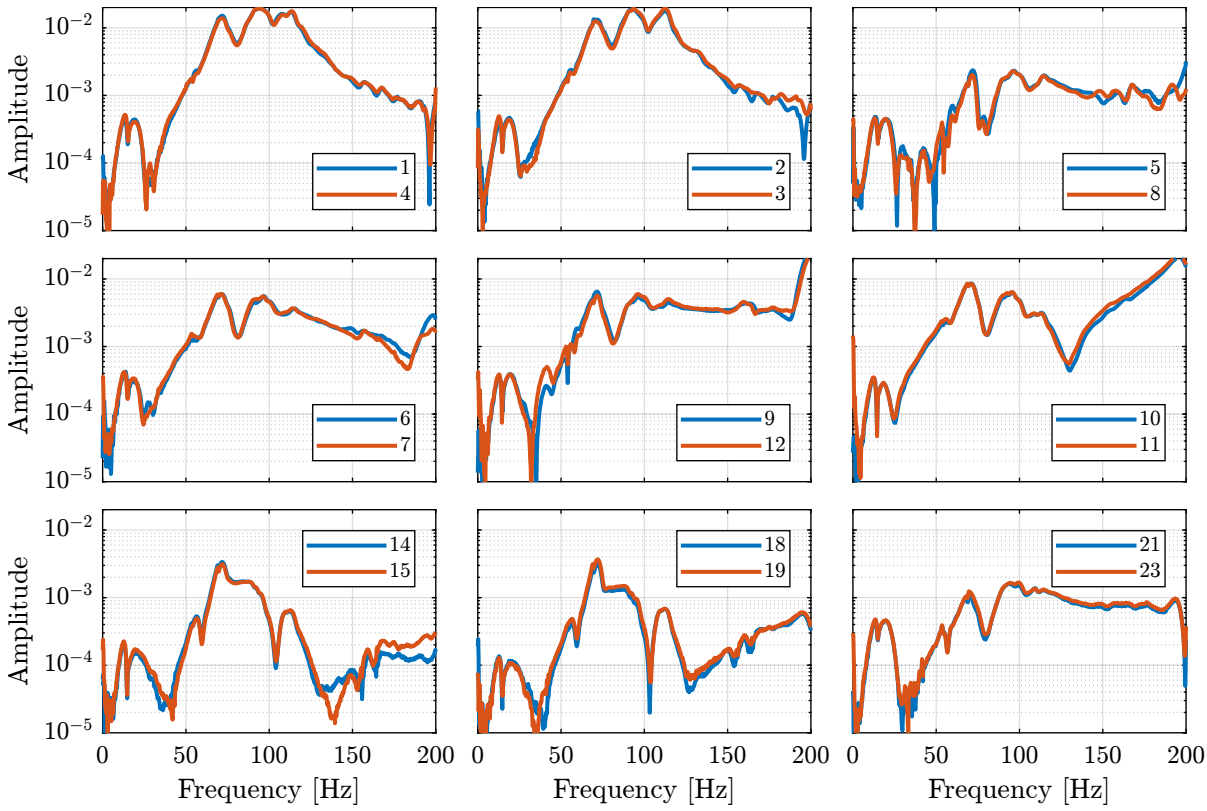

Figure 2.2: Comparaison of measured frequency response function for in the X directions for accelerometers aligned along X. Amplitude is in $\frac{m/s^2}{N}$. Accelerometer number is shown in the legend.

2.2 From accelerometer DOFs to solid body DOFs

Let's consider the schematic shown in Figure 2.3 where the motion of a solid body is measured at 4 distinct locations (in x, y and z directions).

The goal here is to link these $4 \times 3 = 12$ measurements to the 6 DOFs of the solid body expressed in the frame $\{O\}$.

Let's consider the motion of the rigid body defined by its displacement $\delta\vec{p}$ and rotation $\delta\vec{\Omega}$ with respect to the reference frame $\{O\}$.

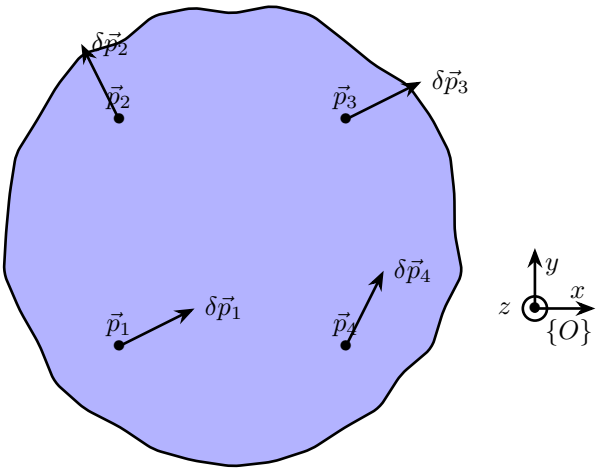

Figure 2.3: Schematic of the measured motions of a solid body

From the figure 2.3, we can write:

$$\begin{aligned}
\delta\vec{p}_1 &= \delta\vec{p} + \boldsymbol{\delta\Omega}\vec{p}_1 \\
\delta\vec{p}_2 &= \delta\vec{p} + \boldsymbol{\delta\Omega}\vec{p}_2 \\
\delta\vec{p}_3 &= \delta\vec{p} + \boldsymbol{\delta\Omega}\vec{p}_3 \\
\delta\vec{p}_4 &= \delta\vec{p} + \boldsymbol{\delta\Omega}\vec{p}_4
\end{aligned}$$

With

$$\boldsymbol{\delta\Omega} = \begin{bmatrix} 0 & -\delta\Omega_z & \delta\Omega_y \\ \delta\Omega_z & 0 & -\delta\Omega_x \\ -\delta\Omega_y & \delta\Omega_x & 0 \end{bmatrix} \tag{2.3}$$

We can rearrange the equations in a matrix form:

$$\left[\begin{array}{ccc|ccc} 1 & 0 & 0 & 0 & p_{1z} & -p_{1y} \\ 0 & 1 & 0 & -p_{1z} & 0 & p_{1x} \\ 0 & 0 & 1 & p_{1y} & -p_{1x} & 0 \\ \hline & \vdots & & & \vdots & \\ \hline 1 & 0 & 0 & 0 & p_{4z} & -p_{4y} \\ 0 & 1 & 0 & -p_{4z} & 0 & p_{4x} \\ 0 & 0 & 1 & p_{4y} & -p_{4x} & 0 \end{array}\right] \left[\begin{array}{c} \delta p_x \\ \delta p_y \\ \delta p_z \\ \hline \delta\Omega_x \\ \delta\Omega_y \\ \delta\Omega_z \end{array}\right] = \left[\begin{array}{c} \delta p_{1x} \\ \delta p_{1y} \\ \delta p_{1z} \\ \hline \vdots \\ \hline \delta p_{4x} \\ \delta p_{4y} \\ \delta p_{4z} \end{array}\right] \tag{2.4}$$

and then we obtain the velocity and rotation of the solid in the wanted frame $\{O\}$:

$$\left[\begin{array}{c} \delta p_x \\ \delta p_y \\ \delta p_z \\ \hline \delta\Omega_x \\ \delta\Omega_y \\ \delta\Omega_z \end{array}\right] = \left[\begin{array}{ccc|ccc} 1 & 0 & 0 & 0 & p_{1z} & -p_{1y} \\ 0 & 1 & 0 & -p_{1z} & 0 & p_{1x} \\ 0 & 0 & 1 & p_{1y} & -p_{1x} & 0 \\ \hline & \vdots & & & \vdots & \\ \hline 1 & 0 & 0 & 0 & p_{4z} & -p_{4y} \\ 0 & 1 & 0 & -p_{4z} & 0 & p_{4x} \\ 0 & 0 & 1 & p_{4y} & -p_{4x} & 0 \end{array}\right]^{-1} \left[\begin{array}{c} \delta p_{1x} \\ \delta p_{1y} \\ \delta p_{1z} \\ \hline \vdots \\ \hline \delta p_{4x} \\ \delta p_{4y} \\ \delta p_{4z} \end{array}\right] \tag{2.5}$$

Important

Using equation (2.5), we can determine the motion of the solid body expressed in a chosen frame $\{O\}$ using the accelerometers attached to it. The inversion is equivalent to resolving a mean square problem.

2.3 Frequency Response Matrix expressed at the Center of Mass

What reference frame to choose? The question we wish here to answer is how to choose the reference frame $\{O\}$ in which the DOFs of the solid bodies are defined.

The possibles choices are:

- **One frame for each solid body** which is located at its center of mass
- **One common frame**, for instance located at the point of interest ($270mm$ above the Hexapod)
- **Base located at the joint position**: this is where we want to see the motion and estimate stiffness

Table 2.1: Advantages and disadvantages for the choice of reference frame

Chosen Frame	Advantages	Disadvantages
Frames at CoM	Physically, it makes more sense	How to compare the motion of the solid bodies?
Common Frame	We can compare the motion of each solid body	Small $\theta_{x,y}$ may result in large $T_{x,y}$
Frames at joint position	Directly gives which joint direction can be blocked	How to choose the joint position?

The choice of the frame depends of what we want to do with the data.

One of the goals is to compare the motion of each solid body to see which relative DOFs between solid bodies can be neglected, that is to say, which joint between solid bodies can be regarded as perfect (and this in all the frequency range of interest). Ideally, we would like to have the same number of degrees of freedom than the number of identified modes.

In the next sections, we will express the FRF matrix in the different frames.

Center of Mass of each solid body From solidworks, we can export the position of the center of mass of each solid body considered. These are summarized in Table 2.2

Computation First, we initialize a new FRF matrix which is an $n \times p \times q$ with:

- n is the number of DOFs of the considered 6 solid-bodies: $6 \times 6 = 36$
- p is the number of excitation inputs: 3
- q is the number of frequency points ω_i

Table 2.2: Center of mass of considered solid bodies

	X [mm]	Y [mm]	Z [mm]
Bottom Granite	45	144	-1251
Top granite	52	258	-778
Translation stage	0	14	-600
Tilt Stage	0	-5	-628
Spindle	0	0	-580
Hexapod	-4	6	-319

Important

For each frequency point ω_i, the FRF matrix is a $n \times p$ matrix:

$$\text{FRF}_{\text{CoM}}(\omega_i) = \begin{bmatrix} \frac{D_{1,T_x}}{F_x}(\omega_i) & \frac{D_{1,T_x}}{F_y}(\omega_i) & \frac{D_{1,T_x}}{F_z}(\omega_i) \\ \frac{D_{1,T_y}}{F_x}(\omega_i) & \frac{D_{1,T_y}}{F_y}(\omega_i) & \frac{D_{1,T_y}}{F_z}(\omega_i) \\ \frac{D_{1,T_z}}{F_x}(\omega_i) & \frac{D_{1,T_z}}{F_y}(\omega_i) & \frac{D_{1,T_z}}{F_z}(\omega_i) \\ \frac{D_{1,R_x}}{F_x}(\omega_i) & \frac{D_{1,R_x}}{F_y}(\omega_i) & \frac{D_{1,R_x}}{F_z}(\omega_i) \\ \frac{D_{1,R_y}}{F_x}(\omega_i) & \frac{D_{1,R_y}}{F_y}(\omega_i) & \frac{D_{1,R_y}}{F_z}(\omega_i) \\ \frac{D_{1,R_z}}{F_x}(\omega_i) & \frac{D_{1,R_z}}{F_y}(\omega_i) & \frac{D_{1,R_z}}{F_z}(\omega_i) \\ \frac{D_{2,T_x}}{F_x}(\omega_i) & \frac{D_{2,T_x}}{F_y}(\omega_i) & \frac{D_{2,T_x}}{F_z}(\omega_i) \\ \vdots & \vdots & \vdots \\ \frac{D_{6,R_z}}{F_x}(\omega_i) & \frac{D_{6,R_z}}{F_y}(\omega_i) & \frac{D_{6,R_z}}{F_z}(\omega_i) \end{bmatrix} \tag{2.6}$$

where 1, 2, ..., 6 corresponds to the 6 solid bodies.

Then, as we know the positions of the accelerometers on each solid body, and we have the response of those accelerometers, we can use the equations derived in the previous section to determine the response of each solid body expressed in their center of mass.

2.4 Verify that we find the original FRF from the FRF in the global coordinates

We have computed the Frequency Response Functions Matrix representing the response of the 6 solid bodies in their 6 DOFs with respect to their center of mass.

From the response of one body in its 6 DOFs, we should be able to compute the FRF of each of its accelerometer fixed to it during the measurement, supposing that this stage is a solid body.

We can then compare the result with the original measurements. This will help us to determine if:

- the previous inversion used is correct
- the solid body assumption is correct in the frequency band of interest

From the translation δp and rotation $\delta\Omega$ of a solid body and the positions p_i of the accelerometers attached to it, we can compute the response that would have been measured by the accelerometers using the following formula:

$$\begin{aligned}\delta p_1 &= \delta p + \delta\Omega p_1\\ \delta p_2 &= \delta p + \delta\Omega p_2\\ \delta p_3 &= \delta p + \delta\Omega p_3\\ \delta p_4 &= \delta p + \delta\Omega p_4\end{aligned}$$

Thus, we can obtain the FRF matrix `FRFs_A` that gives the responses of the accelerometers to the forces applied by the hammer.

It is implemented in matlab as follow: We then compare the original FRF measured for each accelerometer `FRFs` with the "recovered" FRF `FRFs_A` from the global FRF matrix in the common frame.

The FRF for the 4 accelerometers on the Hexapod are compared in Figure 2.4. All the FRF are matching very well in all the frequency range displayed.

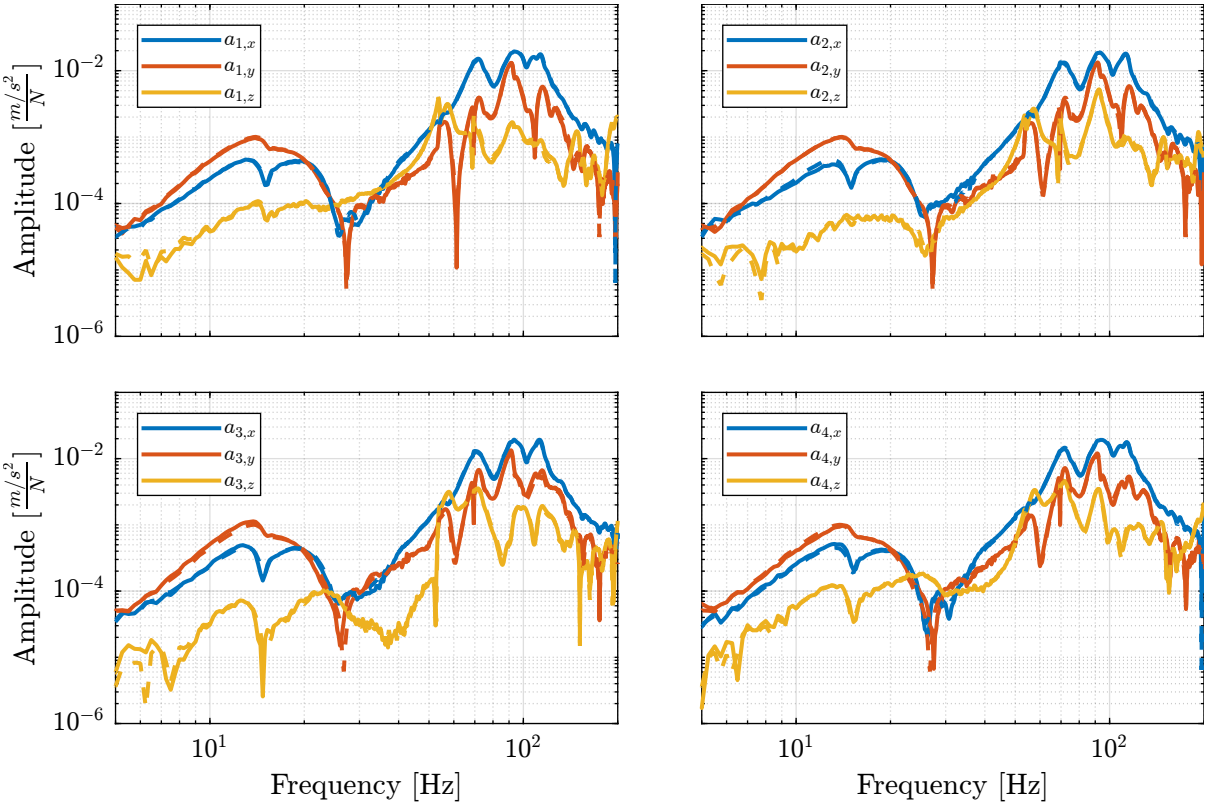

Figure 2.4: Comparaison of the original accelerometer response and reconstructed response from the solid body response. For accelerometers 1 to 4 corresponding to the hexapod.

Important

The reduction of the number of degrees of freedom from 69 (23 accelerometers with each 3DOF) to 36 (6 solid bodies with 6 DOF) seems to work well.
This confirms the fact that the stages are indeed behaving as a solid body in the frequency band

of interest. This valid the fact that a multi-body model can be used to represent the dynamics of the micro-station.

3 Modal Analysis

The goal here is to extract the modal parameters describing the modes of station being studied, namely:

- the eigen frequencies and the modal damping (eigen values)
- the mode shapes (eigen vectors)

This is done from the FRF matrix previously extracted from the measurements.

In order to do the modal parameter extraction, we first have to estimate the order of the modal model we want to obtain. This corresponds to how many modes are present in the frequency band of interest. In section 3.1, we will use the Singular Value Decomposition and the Modal Indication Function to estimate the number of modes.

The modal parameter extraction methods generally consists of **curve-fitting a theoretical expression for an individual FRF to the actual measured data**. However, there are multiple level of complexity:

- works on a part of a single FRF curve
- works on a complete curve encompassing several resonances
- works on a set of many FRF plots all obtained from the same structure

The third method is the most complex but gives better results. This is the one we will use in section 3.2.

From the modal model, it is possible to obtain a graphic display of the mode shapes (section 3.3).

In order to validate the quality of the modal model, we will synthesize the FRF matrix from the modal model and compare it with the FRF measured (section 3.4).

The modes of the structure are expected to be complex, however real modes are easier to work with when it comes to obtain a spatial model from the modal parameters.

3.1 Determine the number of modes

Singular Value Decomposition - Modal Indication Function The Mode Indicator Functions are usually used on $n \times p$ FRF matrix where n is a relatively large number of measurement DOFs and p is the number of excitation DOFs, typically 3 or 4.

In these methods, the frequency dependent FRF matrix is subjected to a singular value decomposition analysis which thus yields a small number (3 or 4) of singular values, these also being frequency dependent.

These methods are used to **determine the number of modes** present in a given frequency range, to **identify repeated natural frequencies** and to pre-process the FRF data prior to modal analysis.

From the documentation of the modal software:

> he MIF consist of the singular values of the Frequency response function matrix. The number of MIFs equals the number of excitations. By the powerful singular value decomposition, the real signal space is separated from the noise space. Therefore, the MIFs exhibit the modes effectively. A peak in the MIFs plot usually indicate the existence of a structural mode, and two peaks at the same frequency point means the existence of two repeated modes. Moreover, the magnitude of the MIFs implies the strength of the a mode.

Important

The **Complex Mode Indicator Function** is defined simply by the SVD of the FRF (sub) matrix:

$$[H(\omega)]_{n\times p} = [U(\omega)]_{n\times n}[\Sigma(\omega)]_{n\times p}[V(\omega)]^H_{p\times p}$$
$$[CMIF(\omega)]_{p\times p} = [\Sigma(\omega)]^T_{p\times n}[\Sigma(\omega)]_{n\times p}$$

We compute the Complex Mode Indicator Function. The result is shown on Figure 3.1.

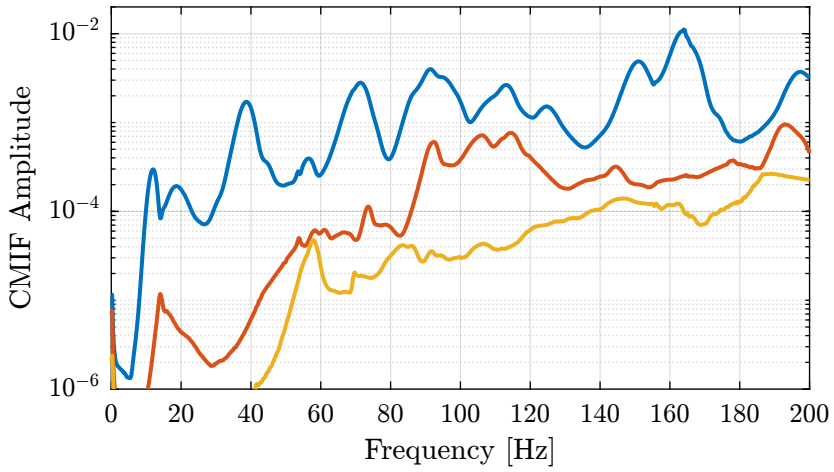

Figure 3.1: Modal Indication Function

Composite Response Function An alternative is the Composite Response Function $HH(\omega)$ defined as the sum of all the measured FRF:

$$HH(\omega) = \sum_j \sum_k H_{jk}(\omega) \tag{3.1}$$

Instead, we choose here to use the sum of the norms of the measured frf:

$$HH(\omega) = \sum_j \sum_k |H_{jk}(\omega)| \tag{3.2}$$

The result is shown on figure 3.2.

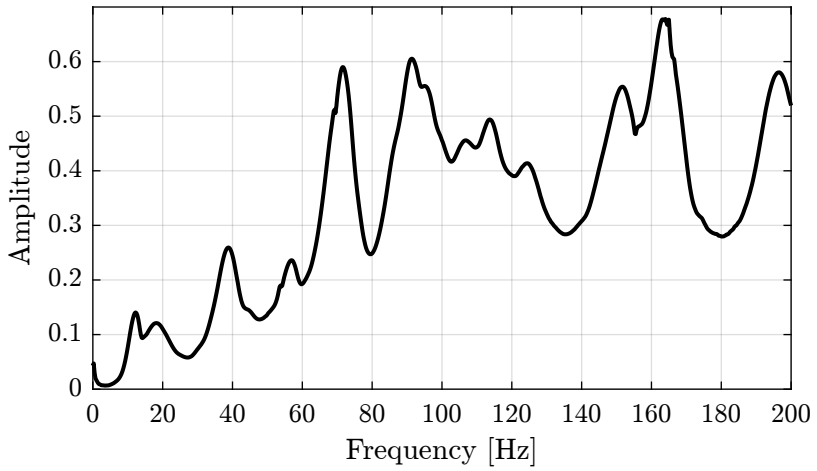

Figure 3.2: Composite Response Function

3.2 Modal parameter extraction

OROS - Modal software Modal identification are done within the Modal software of OROS.

Several modal parameter extraction methods are available. We choose to use the "broad band" method as it permits to identify the modal parameters using all the FRF curves at the same time. It takes into account the fact the the properties of all the individual curves are related by being from the same structure: all FRF plots on a given structure should indicate the same values for the natural frequencies and damping factor of each mode.

Such method also have the advantage of producing a **unique and consistent model** as direct output.

In order to apply this method, we select the frequency range of interest and we give an estimate of how many modes are present.

Then, it shows a stabilization charts, such as the one shown on figure 3.3, where we have to manually select which modes to take into account in the modal model.

We can then run the modal analysis, and the software will identify the modal damping and mode shapes at the selected frequency modes.

Importation of the modal parameters on Matlab The obtained modal parameters are:

- Resonance frequencies in Hertz

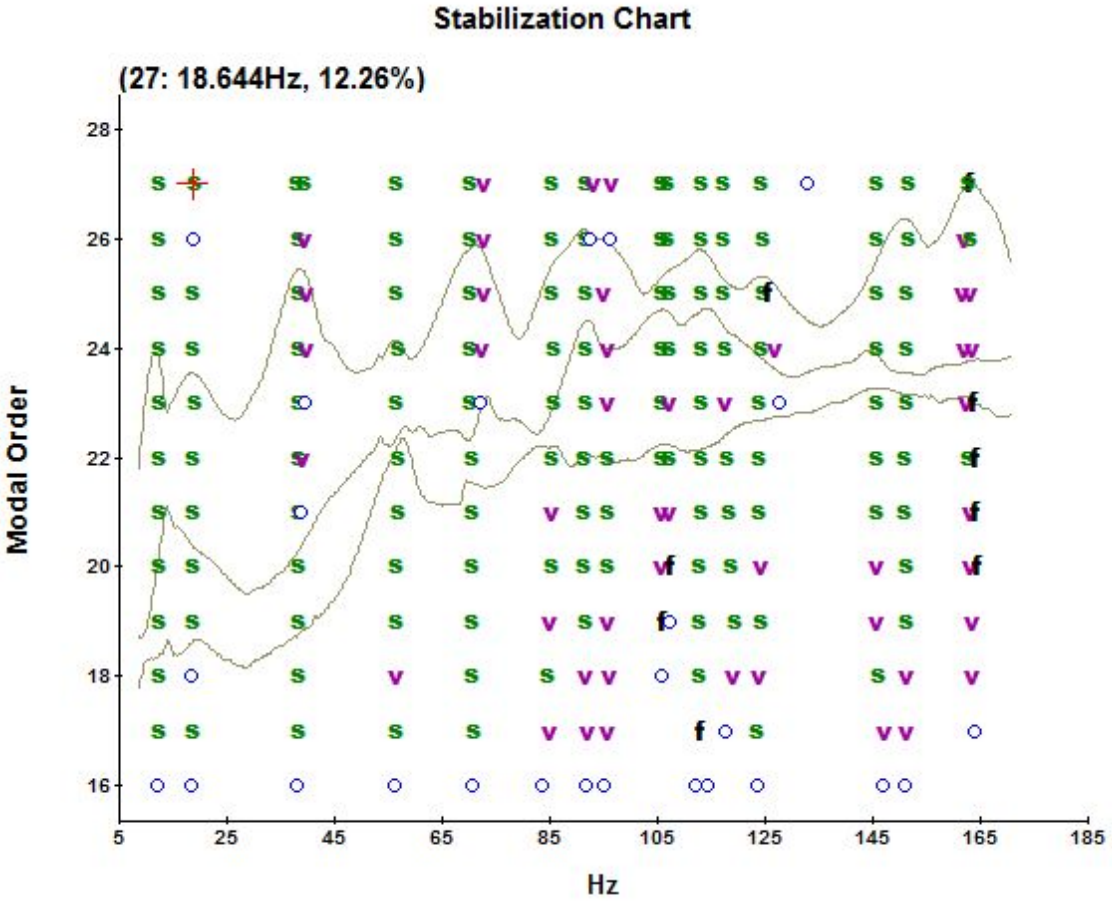

Figure 3.3: Stabilization Chart

- Modal damping ratio in percentage
- (complex) Modes shapes for each measured DoF
- Modal A and modal B which are parameters important for further normalization

The obtained mode frequencies and damping are shown in Table 3.1.

Table 3.1: Obtained eigen frequencies and modal damping

Mode	Frequency [Hz]	Damping [%]
1	11.9	12.2
2	18.6	11.7
3	37.8	6.2
4	39.1	2.8
5	56.3	2.8
6	69.8	4.3
7	72.5	1.3
8	84.8	3.7
9	91.3	2.9
10	105.5	3.2
11	106.6	1.6
12	112.7	3.1
13	124.2	2.8
14	145.3	1.3
15	150.5	2.4
16	165.4	1.4

Theory It seems that the modal analysis software makes the **assumption** of viscous damping for the model with which it tries to fit the FRF measurements.

If we note N the number of modes identified, then there are $2N$ eigenvalues and eigenvectors given by the software:

$$s_r = \omega_r(-\xi_r + i\sqrt{1-\xi_r^2}), \quad s_r^* \tag{3.3}$$

$$\{\psi_r\} = \begin{Bmatrix} \psi_{1_x} & \psi_{2_x} & \dots & \psi_{23_x} & \psi_{1_y} & \dots & \psi_{1_z} & \dots & \psi_{23_z} \end{Bmatrix}^T, \quad \{\psi_r\}^* \tag{3.4}$$

for $r = 1, \dots, N$ where ω_r is the natural frequency and ξ_r is the critical damping ratio for that mode.

Modal Matrices We would like to arrange the obtained modal parameters into two modal matrices:

$$\Lambda = \begin{bmatrix} s_1 & & 0 \\ & \ddots & \\ 0 & & s_N \end{bmatrix}_{N\times N}; \quad \Psi = \begin{bmatrix} & & \\ \{\psi_1\} & \dots & \{\psi_N\} \\ & & \end{bmatrix}_{M\times N}$$

$$\{\psi_i\} = \begin{Bmatrix} \psi_{i,1_x} & \psi_{i,1_y} & \psi_{i,1_z} & \psi_{i,2_x} & \dots & \psi_{i,23_z} \end{Bmatrix}^T$$

M is the number of DoF: here it is $23 \times 3 = 69$. N is the number of mode

Each eigen vector is normalized: $\|\{\psi_i\}\|_2 = 1$

However, the eigen values and eigen vectors appears as complex conjugates:

$$s_r, s_r^*, \{\psi\}_r, \{\psi\}_r^*, \quad r = 1, N$$

(a) Mode 1

(b) Mode 6

(c) Mode 13

Figure 3.4: Instrumentation used for the modal analysis

In the end, they are $2N$ eigen values. We then build two extended eigen matrices as follow:

$$\mathcal{S} = \begin{bmatrix} s_1 & & & & & \\ & \ddots & & & 0 & \\ & & s_N & & & \\ & & & s_1^* & & \\ & 0 & & & \ddots & \\ & & & & & s_N^* \end{bmatrix}_{2N \times 2N} \quad ; \quad \Phi = \begin{bmatrix} \{\psi_1\} & \dots & \{\psi_N\} & \{\psi_1^*\} & \dots & \{\psi_N^*\} \end{bmatrix}_{M \times 2N}$$

We also build the Modal A and Modal B matrices:

$$A = \begin{bmatrix} a_1 & & 0 \\ & \ddots & \\ 0 & & a_N \end{bmatrix}_{N \times N} \quad ; \quad B = \begin{bmatrix} b_1 & & 0 \\ & \ddots & \\ 0 & & b_N \end{bmatrix}_{N \times N} \tag{3.5}$$

With a_i is the "Modal A" parameter linked to mode i.

"Modal A" and "modal B" are linked through the following formula:

$$B = -A\Lambda$$

3.3 Obtained Mode Shapes animations

From the modal parameters, it is possible to show the modal shapes with an animation.

Examples are shown in Figures 3.4.

We can learn quite a lot from these mode shape animations.

For instance, the mode shape of the first mode at 11Hz (figure 3.4a) seems to indicate that this corresponds to a suspension mode.

This could be due to the 4 Airloc Levelers that are used for the granite (figure 3.5).

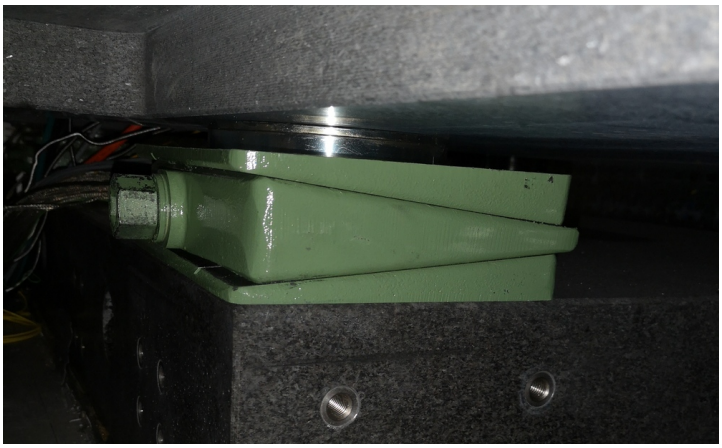

Figure 3.5: AirLoc used for the granite (2120-KSKC)

They are probably **not well leveled**, so the granite is supported only by two Airloc.

3.4 Verify the validity of the Modal Model

There are two main ways to verify the validity of the modal model

- Synthesize FRF measurements that has been used to generate the modal model and compare
- Synthesize FRF that has not yet been measured. Then measure that FRF and compare

From the modal model, we want to synthesize the Frequency Response Functions that has been used to build the modal model.

Let's recall that:

- M is the number of measured DOFs ($3 \times n_{\text{acc}}$)
- N is the number of modes identified

We then have that the FRF matrix $[H_{\text{syn}}]$ can be synthesize using the following formula:

Important

$$[H_{\text{syn}}(\omega)]_{M\times M} = [\Phi]_{M\times 2N} \left[\frac{Q_r}{j\omega - s_r}\right]_{2N\times 2N} [\Phi]^T_{2N\times M} \tag{3.6}$$

with $Q_r = 1/M_{A_r}$

An alternative formulation is:

$$H_{pq}(s_i) = \sum_{r=1}^{N} \frac{A_{pqr}}{s_i - \lambda_r} + \frac{A^*_{pqr}}{s_i - \lambda^*_r}$$

with:

- $A_{pqr} = \frac{\psi_{pr}\psi_{qr}}{M_{A_r}}$, M_{A_r} is called "Modal A"
- ψ_{pr}: scaled modal coefficient for output DOF p, mode r
- λ_r: complex modal frequency

From the modal software documentation:

> Modal A Scaling constant for a complex mode. It has the same properties as modal mass for normal modes (undamped or proportionally damped cases). Assuming
>
> - ψ_{pr} = Modal coefficient for measured degree of freedom p and mode r
> - ψ_{qr} = Modal coefficient for measured degree of freedom q and mode r
> - A_{pqr} = Residue for measured degree of freedom p, measured degree of q and mode r
> - M_{Ar} = Modal A of mode r
>
> Then
>
> $$A_{pqr} = \frac{\psi_{pr}\psi_{qr}}{M_{Ar}}$$
>
> **Modal B** Scaling constant for a complex mode. It has the same properties as modal stiffness for normal modes (undamped or proportionally damped cases). Assuming
>
> - M_{Ar} = Modal A of mode r
> - λ_r = System pole of mode r
>
> Then
>
> $$M_{Br} = -\lambda_r M_{Ar}$$

The comparison between the original measured frequency response function and the synthesized one from the modal model is done in Figure 3.6.

Frequency response functions that has not been measured can be synthesized as shown in Figure 3.7.

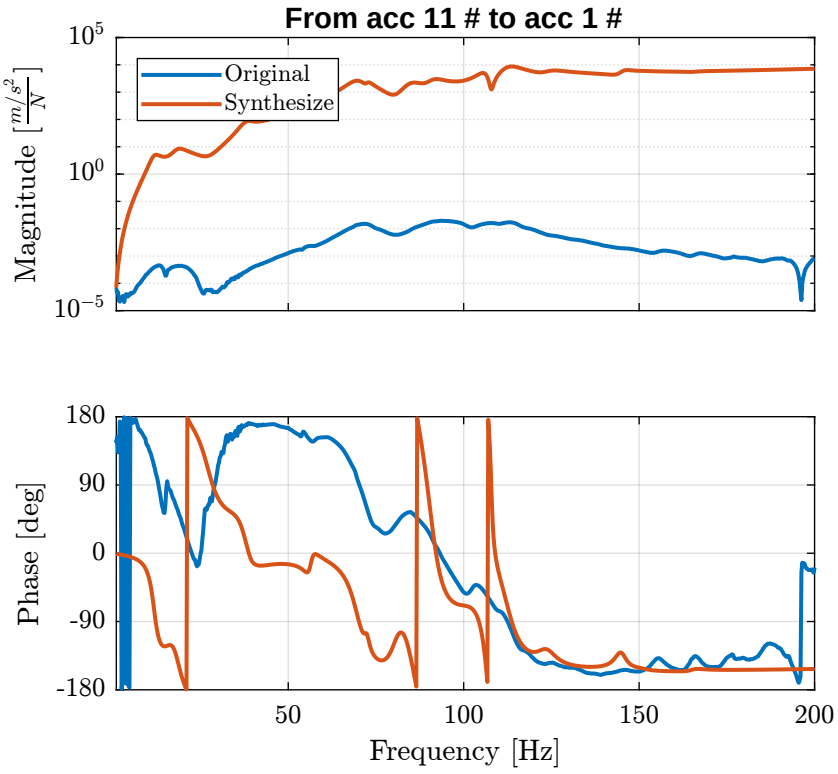

Figure 3.6: description

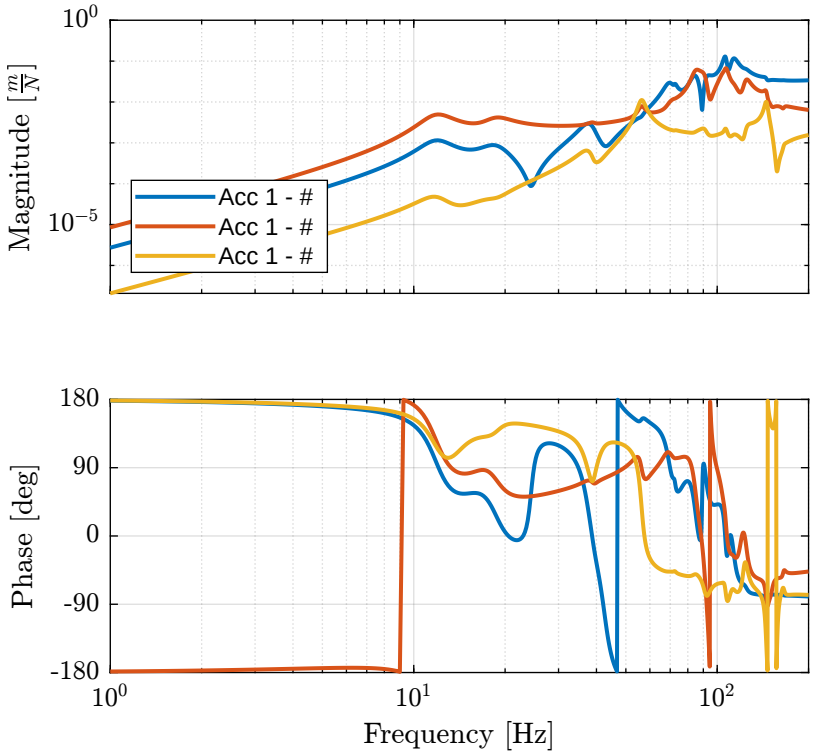

Figure 3.7: description

4 Conclusion

Validation of solid body model.

Further step: go from modal model to parameters of the solid body model.

Bibliography

[1] D. Ewins, *Modal testing: theory, practice and application*. Baldock, Hertfordshire, England Philadelphia, PA: Wiley-Blackwell, 2000, pp. 978–0 863 802 188 (cit. on pp. 3, 8).